3D Registration with Maximal Cliques
Supplementary Material

Xiyu Zhang Jiaqi Yang* Shikun Zhang Yanning Zhang
School of Computer Science, Northwestern Polytechnical University, China
{2426988253, zhangshikun}@mail.nwpu.edu.cn; {jqyang, ynzhang}@nwpu.edu.cn

A. Comparison of FOG and SOG

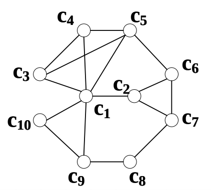

	C_1	C_2	C_3	C_4	C_5	C_6	C_7	C_8	C_9	C_{10}
C_1	0	0.91	0.93	0.92	0.95	0	0	0	0.9	0.91
C_2	0.91	0	0	0	0	0.95	0.94	0	0	0
C_3	0.93	0	0	0.93	0.96	0	0	0	0	0
C_4	0.92	0	0.93	0	0.95	0	0	0	0	0
C_5	0.95	0	0.96	0.95	0	0.92	0	0	0	0
C_6	0	0.95	0	0	0.92	0	0.95	0	0	0
C_7	0	0.94	0	0	0	0.95	0	0.91	0	0
C_8	0	0	0	0	0	0	0.91	0	0.94	0
C_9	0.9	0	0	0	0	0	0	0.94	0	0.96
C_{10}	0.91	0	0	0	0	0	0	0	0.96	0

(a)

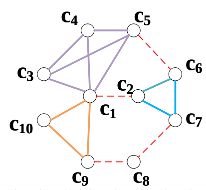

	C_1	C_2	C_3	C_4	C_5	C_6	C_7	C_8	C_9	C_{10}
C_1	0	0	1.64	1.63	1.68	0	0	0	0.79	0.79
C_2	0	0	0	0	0	0.85	0.85	0	0	0
C_3	1.64	0	0	1.64	1.7	0	0	0	0	0
C_4	1.63	0	1.64	0	1.68	0	0	0	0	0
C_5	1.68	0	1.7	1.68	0	0	0	0	0	0
C_6	0	0.85	0	0	0	0	0.85	0	0	0
C_7	0	0.85	0	0	0	0.85	0	0	0	0
C_8	0	0	0	0	0	0	0	0	0	0
C_9	0.79	0	0	0	0	0	0	0	0	0.79
C_{10}	0.79	0	0	0	0	0	0	0	0.79	0

(b)

Figure 1. An example that illustrates the relationship between FOG and SOG. (**a**) FOG and its weight matrix. (**b**) SOG and its weight matrix.

As shown in Fig. 1: 1) SOG considers the commonly compatible matches in the global set of the matched pairs rather than only the geometric consistency, making it more consistent and more robust in the case of high outlier rates; 2) SOG is sparser than FOG, and therefore beneficial in making the search of cliques more rapid.

The weights of the edge $e_{ij} = (\mathbf{c}_i, \mathbf{c}_j)$ in the FOG are transformed as follows to obtain the corresponding second-order weights:

$$w_{SOG}(e_{ij}) = w_{FOG}(e_{ij}) \cdot \sum_{\substack{e_{ik}\in\mathbf{E} \\ e_{jk}\in\mathbf{E}}} \left[w_{FOG}(e_{ik}) \cdot w_{FOG}(e_{jk}) \right]. \tag{1}$$

If no remaining nodes form edges with both $\mathbf{c}_i$ and $\mathbf{c}_j$, $w_{SOG}(e_{ij})$ will be 0, which demonstrates that e_{ij} will be removed from SOG then. In Fig. 1(b), the four edges e_{12}, e_{56}, e_{78} and e_{89} are removed, and the whole graph is divided into subgraphs that contain several cliques naturally.

*Corresponding author.

B. Additional Experiments

The information of all tested datasets is presented in Table 1.

Results on ETH. Additionally, we also test our method on the outdoor dataset ETH [6], which contains more complex geometries compared with 3DMatch [8]. FPFH [7], FCGF [2], and Spinnet [1] are employed to generate correspondences, from which registration will then be performed by RANSAC-50K and MAC. The number of sampled points or correspondences is set to 5000. Registration is considered successful when the RE $\leq$ 15°and TE $\leq$ 30 cm. The quality of generated correspondence and registration results are reported in Table 2 and Table 3, respectively.

The results suggest that when a defect in a descriptor leads to a very low inlier rate for generating the correspondence set, MAC is still effective in finding the accurate consistent subset from it, thus greatly boosting the registration recall. The registration recall obtained by using MAC is 24.2% higher than RANSAC when combined with FPFH, and 18.51% higher when combined with FCGF. MAC working with Spinnet achieves a registration recall of **94.67%** on ETH.

Time and memory analysis. Efficiency and memory consumption results of several well-performed methods are shown in Tables 4 and 5, respectively. Regarding efficiency experiments, all methods have been tested for ten rounds, and the mean and standard deviation results are reported. All methods were executed in the CPU. The results indicate that MAC is quite lightweight and efficient when the input correspondence number is less than 2.5k.

C. Visualizations

We show more registration results in Figs. 2-5.

Dataset	Data type	Nuisances	Application scenario	# Matching pairs
U3M [5]	Object	Limited overlap, self-occlusion	Registration	496
3DMatch [8]	Indoor scene	Occlusion, real noise	Registration	1623
3DLoMatch [4]	Indoor scene	Limited overlap, occlusion, real noise	Registration	1781
KITTI [3]	Outdoor scene	Clutter, occlusion, real noise	Detection, registration, segmentation	555
ETH [6]	Outdoor scene	Limited overlap, clutter, occlusion, real noise	Feature description, registration	713

Table 1. Information of all tested datasets.

	Gazebo		**Wood**		Avg.
	Autumn	Summer	Autumn	Summer	
FPFH [7]	0.42	0.24	0.21	0.26	0.29
FCGF [2]	2.34	1.25	1.35	1.68	1.62
Spinnet [1]	16.67	13.73	12.20	14.67	14.40

Table 2. Inlier ratio (%) of generated correspondence on ETH dataset.

	Gazebo		**Wood**		Avg.
	Autumn	Summer	Autumn	Summer	
FPFH [7]	16.85	10.03	10.43	10.40	11.92
FCGF [2]	54.35	28.03	52.17	51.20	42.78
Spinnet [1]	98.37	83.05	100.00	99.20	92.57
FPFH+MAC	46.74	27.68	33.04	43.20	36.12
	29.89↑	17.65↑	22.61↑	32.80↑	24.20↑
FCGF+MAC	75.54	42.91	71.30	73.60	61.29
	21.19↑	14.88↑	19.13↑	22.40↑	18.51↑
Spinnet+MAC	98.91	87.54	100.00	100.00	94.67
	0.54↑	4.49↑	-	0.80↑	2.10↑

Table 3. Registration recall (%) boosting for various descriptors combined with MAC on ETH dataset.

# Corr.	250	500	1000	2500	5000
PointDSC	32.24±0.81	78.38±0.89	240.46±2.18	1401.97±12.24	5504.11±10.32
TEASER++	6.40±1.88	6.68±0.66	16.74±1.21	104.24±0.53	484.93±1.87
SC^2-PCR	19.34±0.63	63.23±0.55	215.98±1.24	1282.73±4.05	5210.17±8.30
MAC	7.32±0.55	23.32±0.38	56.45±1.41	282.67±7.83	3259.38±12.66

Table 4. Comparisons on average time consumption (ms).

# Corr.	250	500	1000	2500	5000
PointDSC	3531.46	3538.26	3582.57	3634.22	3736.10
TEASER++	1631.92	1634.77	2029.22	2266.84	2484.83
SC^2-PCR	448.01	453.18	508.40	621.27	690.22
MAC	15.59	17.43	23.49	52.79	150.86

Table 5. Comparisons on average memory consumption (MB).

References

[1] Sheng Ao, Qingyong Hu, Bo Yang, Andrew Markham, and Yulan Guo. Spinnet: Learning a general surface descriptor for 3d point cloud registration. In *Proceedings of the IEEE/CVF Conference on Computer Vision and Pattern Recognition*, pages 11753–11762, 2021. 1, 2

[2] Christopher Choy, Jaesik Park, and Vladlen Koltun. Fully convolutional geometric features. In *Proceedings of the IEEE/CVF International Conference on Computer Vision*, pages 8958–8966, 2019. 1, 2

[3] Andreas Geiger, Philip Lenz, and Raquel Urtasun. Are we ready for autonomous driving? the kitti vision benchmark suite. In *Proceedings of the IEEE Conference on Computer Vision and Pattern Recognition*, pages 3354–3361. IEEE, 2012. 2

[4] Shengyu Huang, Zan Gojcic, Mikhail Usvyatsov, Andreas Wieser, and Konrad Schindler. Predator: Registration of 3d point clouds with low overlap. In *Proceedings of the IEEE/CVF Conference on Computer Vision and Pattern Recognition*, pages 4267–4276, 2021. 2

[5] Ajmal S Mian, Mohammed Bennamoun, and Robyn A Owens. A novel representation and feature matching algorithm for automatic pairwise registration of range images. *International Journal of Computer Vision*, 66(1):19–40, 2006. 2

[6] François Pomerleau, Ming Liu, Francis Colas, and Roland Siegwart. Challenging data sets for point cloud registration algorithms. *The International Journal of Robotics Research*, 31(14):1705–1711, 2012. 1, 2

[7] Radu Bogdan Rusu, Nico Blodow, and Michael Beetz. Fast point feature histograms (fpfh) for 3d registration. In *IEEE International Conference on Robotics and Automation*, pages 3212–3217. IEEE, 2009. 1, 2

[8] Andy Zeng, Shuran Song, Matthias Nießner, Matthew Fisher, Jianxiong Xiao, and Thomas Funkhouser. 3dmatch: Learning local geometric descriptors from rgb-d reconstructions. In *Proceedings of the IEEE Conference on Computer Vision and Pattern Recognition*, pages 1802–1811, 2017. 1, 2

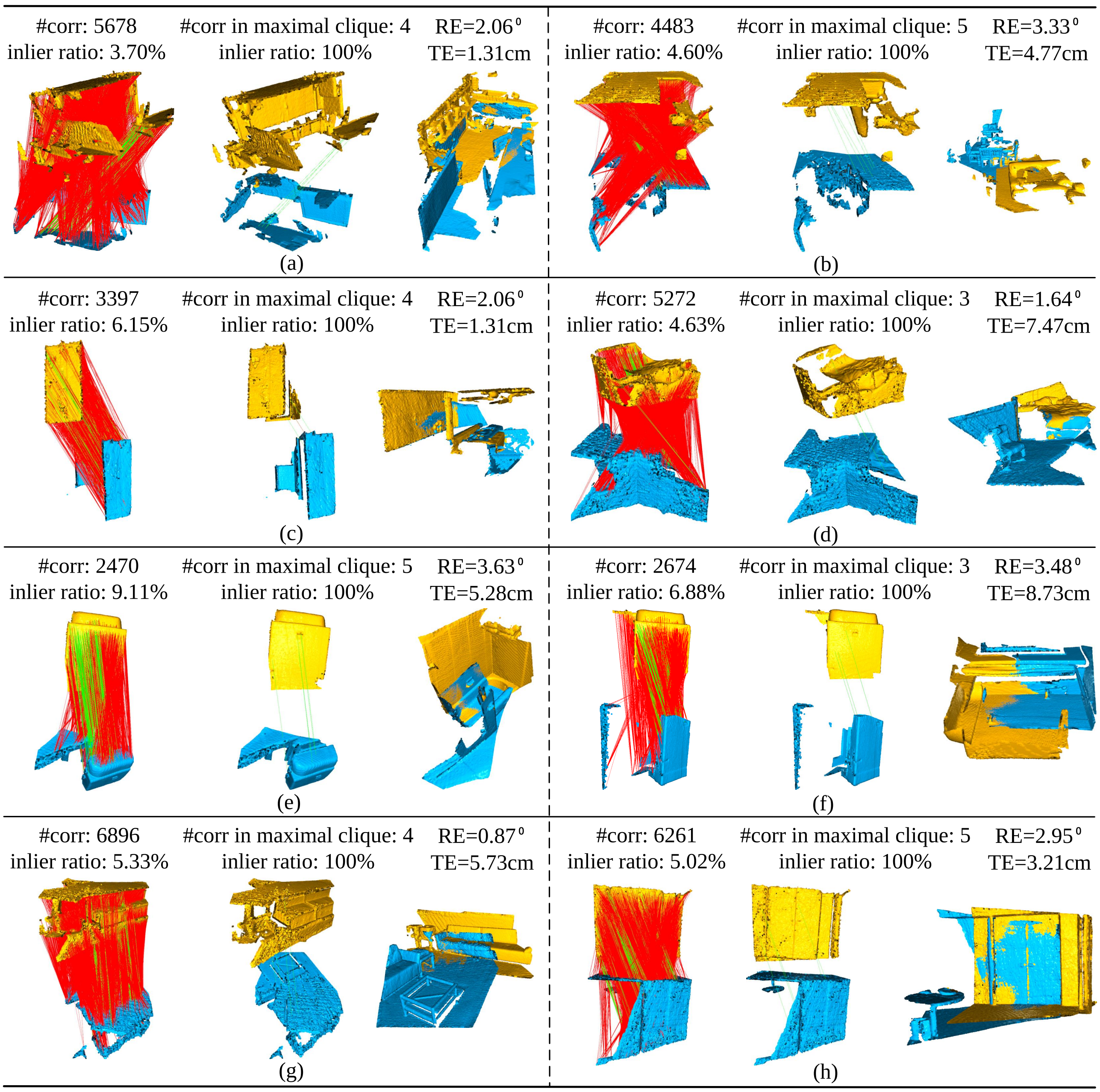

Figure 2. Registration process-visualizations of MAC on 3DMatch.

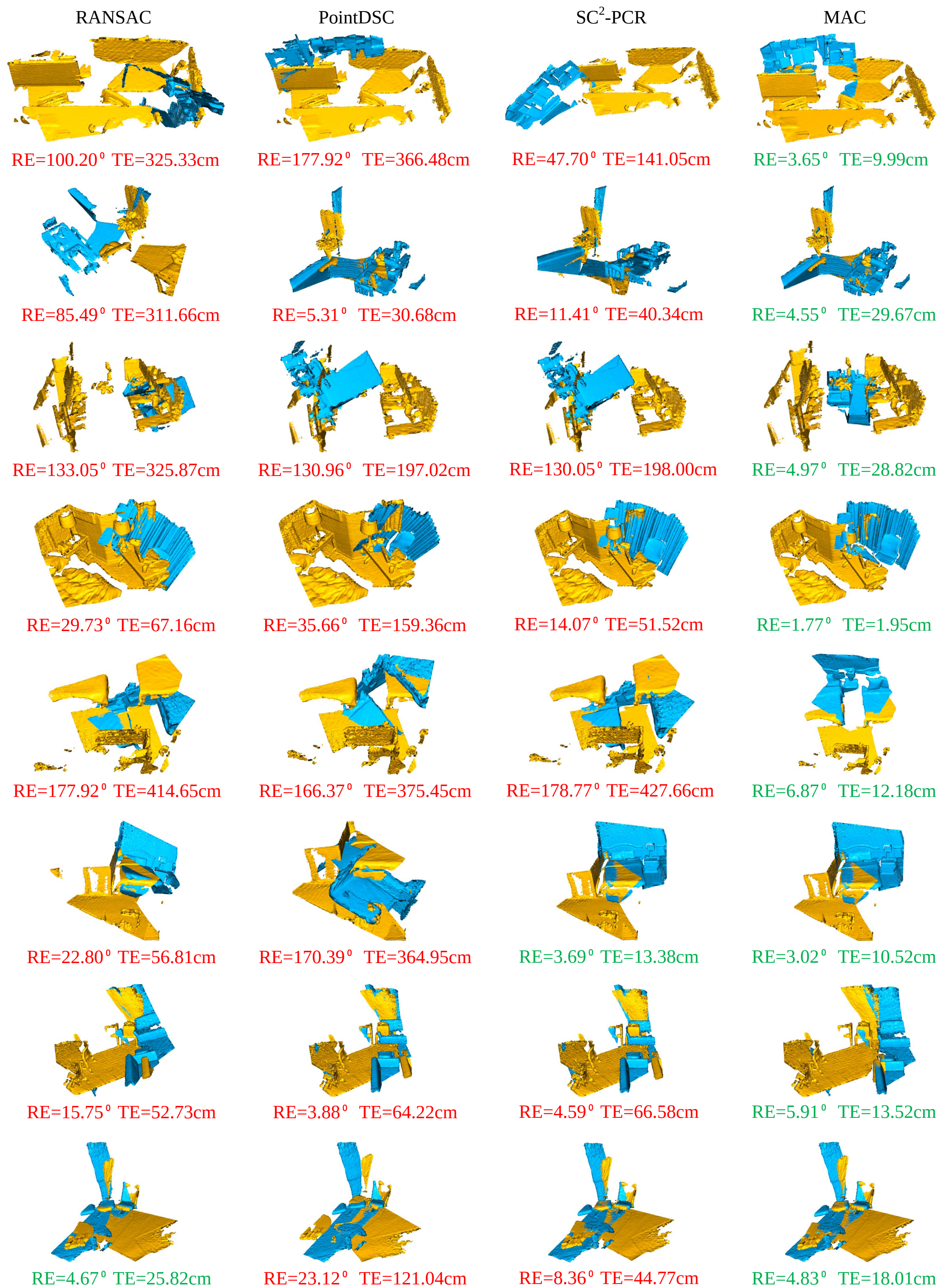

Figure 3. Qualitative comparison on 3DLoMatch. Red and green represent failed and successful registration, respectively.

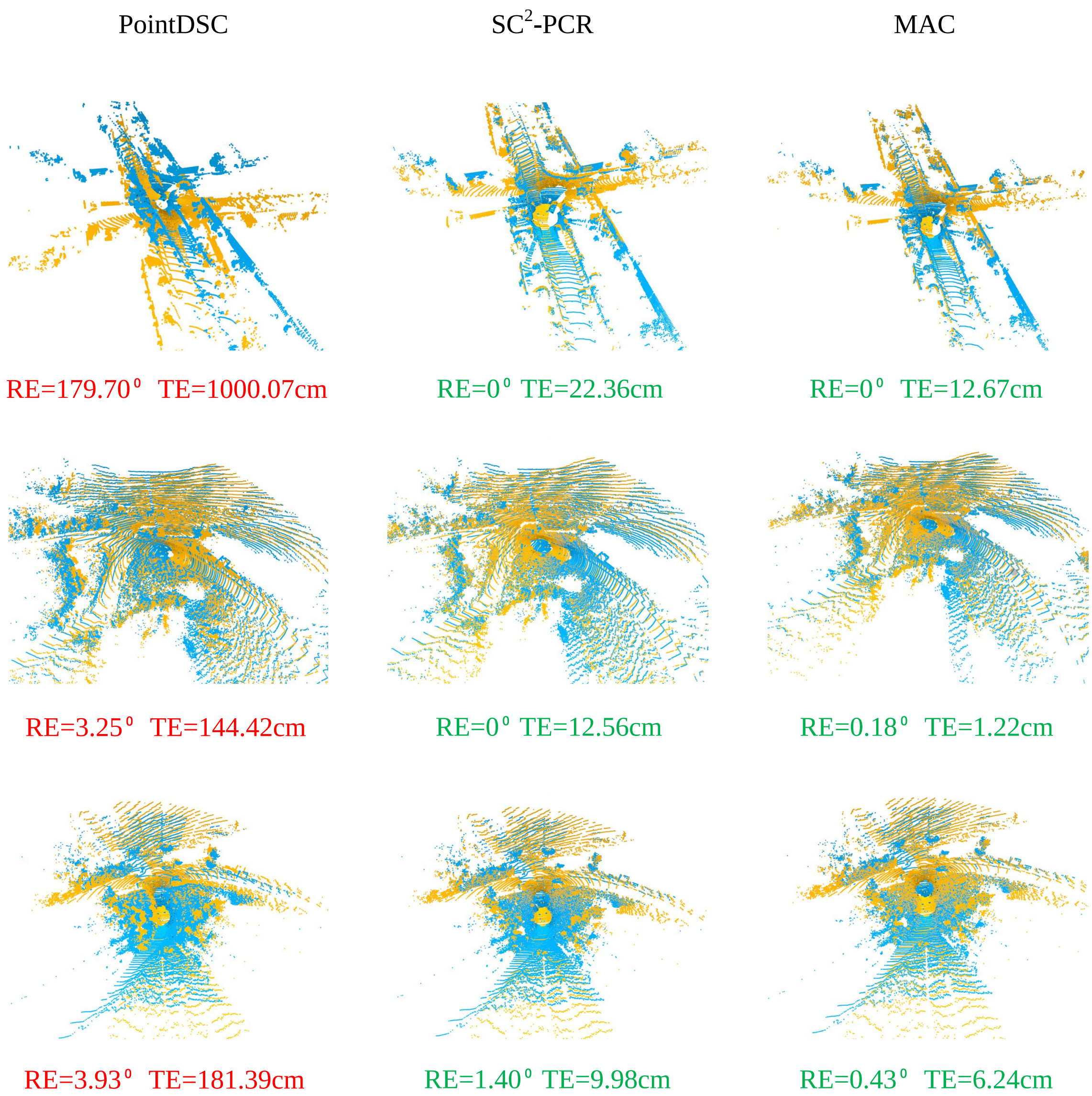

Figure 4. Qualitative comparison on KITTI.

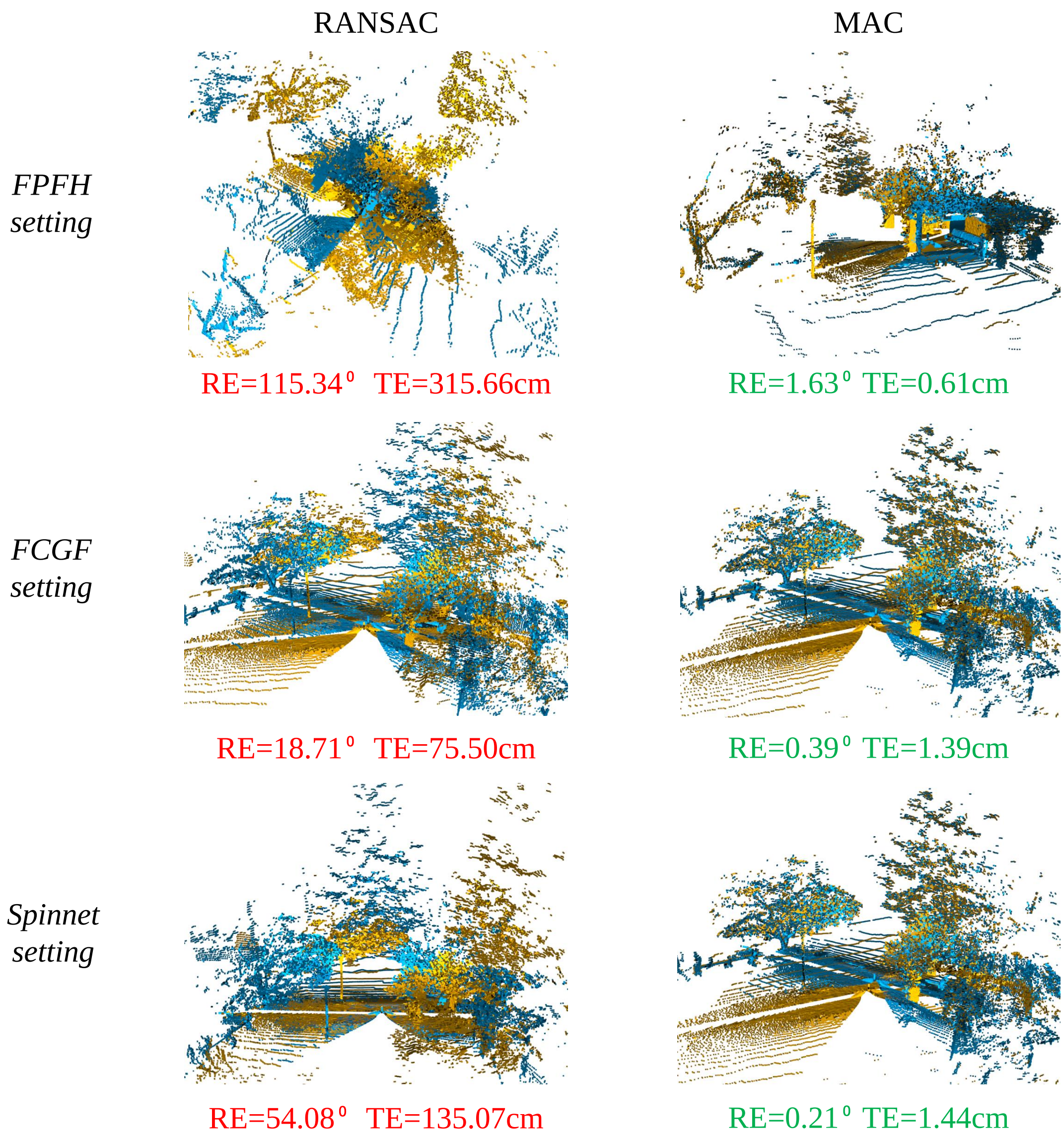

Figure 5. Qualitative comparison on ETH.